Preprints, 4th IFAC Conference on
Advances in Proportional-Integral-Derivative Control
Almería, Spain | June 12-14, 2024

Hierarchical Model-Based Irrigation Control for Vertical Farms

Annalena Daniels [*,1] **Michael Fink** [*,1] **Dirk Wollherr** [*]

[*] *Chair of Automatic Control Engineering, Technical University of Munich, Germany, {a.daniels, michael.fink, dirk.wollherr}@tum.de*

Abstract: As high energy costs and water scarcity remain major problems in the context of vertical farming, we present a hierarchical control system developed for the optimization of irrigation processes in these farms. The main objective is to minimize the energy cost and water consumption associated with the operation of a vertical farm, with special emphasis on irrigation in a soil-based environment. At a higher level, an optimal control problem based on a dynamic crop growth model and the FAO Penman-Monteith equations is solved offline to determine the optimal daily inputs, considering temperature, radiation, and plant available water as decision variables. At a lower level, strategically placed Proportional-Integral-Derivative (PID) controllers are used to track these irrigation set-points online. These controllers are designed using a dynamic drip irrigation and soil model that simulates the movement of water through soil. In a simulation study, this integration of set-points and subordinate PID controllers shows a robust control system that effectively stabilizes the irrigation process. The results also show a uniform moisture distribution in the soil after a short time, which contributes to uniform plant growth in the farm. The proposed hierarchical control system combines computationally intensive offline open-loop optimization for daily input determination with fast and simple online PID control for real-time stabilization.

Keywords: Greenhouse control, Modeling and control of agriculture, Applications of PID control, Optimal control, Vertical farming

1. INTRODUCTION

With the increasing demand for food from the world's growing population and water scarcity due to climate change, there is an urgent need to re-evaluate agricultural practices. Relying solely on conventional farming methods to ensure future food security is fraught with risk. This is why scientists have been researching smart agriculture for decades, and much important work has already been published and implemented (Hassan et al., 2021). Smart agriculture uses advances in weather forecasting and the optimization of input parameters to increase the efficiency of crop production. While the optimization potential is also applicable in field cultivation, it increases significantly in controlled environments such as greenhouses. An even more sophisticated variant, known as vertical farming, represents a paradigm shift in producing high-quality food in completely enclosed spaces and minimizes dependence on pesticides and harmful chemicals. This approach, characterized by resource efficiency and fine-tuning through mathematical models and algorithms, is a promising approach to sustainable agriculture. The biggest problem, however, is the enormous energy consumption on these farms (Graamans et al., 2018), which makes widespread application in practice untenable to date. For this reason, it is absolutely essential to minimize energy consumption and use the available resources as efficiently as possible.

One of the components of a vertical farm (VF) is automatic irrigation, the input of which is highly dependent on other parameters such as temperature and radiation. Optimizing irrigation for crop growth therefore requires both a model of plant growth and one of the medium that carries the water. In classical agriculture, soil is used as a medium. Thus, there are many models for water movement in soil (Kirkham, 2023; Romashchenko et al., 2016). Even though most VFs are designed as hydroponic systems, recent studies emphasize the nuanced effects of soil-less systems on plant health. For certain crops, soil-based vertical farming remains an important consideration due to its potential advantages over hydroponic or aquaponic systems (Bender et al., 2016). Current knowledge highlights the complex interactions between plants and their soil microbiome, contributing to improved nutrient uptake and overall plant resilience (Trivedi et al., 2020). While recognizing the benefits, it is important to acknowledge the inherent challenge of soil-based systems, which is primarily that the soil contains pathogens and therefore needs to be disinfected. While this paper focuses on soil-based systems, hydroponic systems can be considered with the same approach after experimental parameterization of the substrate parameters for the model.

Automated irrigation in the context of smart farming has received considerable attention in recent years. For example, Puig et al. (2022) have developed a platform for outdoor drip irrigation systems that integrates an open IoT application with a versatile architecture that enables connectivity to various sensors and agronomic models. In an effort to evaluate the uniformity of water distribution in the soil for different types of drip irrigation, Muñoz-Carpena and Dukes (2005) focused on the pipe flow process within a drip irrigation unit in a real field.

[1] These authors contributed equally to this work.

Another strategy involves using soil moisture sensors that turn irrigation on or off based on readings that exceed or fall below predefined thresholds (Cáceres et al., 2007).

The implementation of a proportional-integral-derivative (PID) controller for automatic irrigation, with no particular focus on optimal crop growth or on uniform distribution, has been investigated in several papers (Sheikh et al., 2018; Romero, 2011; Romero et al., 2012). A more sophisticated approach is presented by Abioye et al. (2023), who developed a Kalman filter PID (KF-PID) controller for fibrous capillary irrigation using a data-driven state-space model. However, this approach requires a significant amount of high-quality data. In the context of optimal irrigation strategies, a predictive controller aimed at maximizing agricultural yield and water conservation was proposed, but without focusing on a uniform distribution of moisture or considering plant growth as a dynamic system (Ortega Álvarez et al., 2004; Cáceres et al., 2021). Rodríguez et al. (2015) integrated water dynamics and plant growth into a joint model in a greenhouse. However, the model neglected any spatial component of water dynamics in the substrate assuming a uniform moisture distribution.

In contrast to existing literature, our paper aims to demonstrate that employing a straightforward PID controller in a hierarchical control scheme can effectively achieve a uniform moisture distribution in soil within a short time and therefore contribute to optimal and uniform plant growth in a VF. This capability allows the system to seamlessly track the daily optimal set-points for plant-available water, i.e., the amount of water that can be extracted from the soil by the plant, which is generally not equal to the total water content of the soil. The plant-available water is obtained from a separate optimal control problem (OCP). This approach of hierarchical irrigation control, to the best of our knowledge, remains unexplored in prior research, though it has been recommended as a promising strategy by Romero et al. (2012).

Our key contributions can be summarized as follows:

- Adaptation of plant and soil models for indoor VFs.
- Offline identification of the optimal daily amount of plant-available water, taking into account optimized values for radiation and temperature within a VF using a dynamic crop growth model.
- Implementation of a PID controller to track the identified set-points, facilitating the determination of a daily optimal drip irrigation scheme.

The remainder of the paper is structured as follows. Section 2 presents the theoretical plant models used for the optimization, as well as the drip irrigation and soil model. In Section 3, hierarchical set-point irrigation control is discussed, and in Section 4, it is evaluated using a simulation example. Section 5 leads the reader through a brief discussion of the results, and Section 6 concludes our work.

2. MODELS

2.1 Dynamic Crop Growth Model in a Vertical Farm

In order to simulate crop growth, the smooth discrete-time state-space reformulation of the SIMPLE model (Zhao et al., 2019) is used, details of which can be found in our previous work (Daniels et al., 2023). The parameters of the SIMPLE model were calibrated carefully using a large arable farming experimental data set for various crops (Zhao et al., 2019) which we adopted in this work. This model is a generic dynamic crop growth model, which means it can be used for several different crops and cultivars if a set of crop-specific parameters is known. The model was found to be very accurate in comparison to other crop models in an optimal control framework (Fink et al., 2023). The state vector for day i is then given as $\boldsymbol{x}_i = [m_{B,i}\ \tau_i\ I_{50B,i}]^\mathsf{T}$, where $m_{B,i}$ is the biomass, τ_i the cumulative temperature and $I_{50B,i}$ the leaf senescence on day i. In contrast to other models, diurnal and nocturnal temperatures are not distinguished and only enter as an average. Under the assumption of a fully controllable environment such as a VF, the system inputs are $\boldsymbol{u}_i = [\vartheta_i\ p_{\mathrm{PAW},i}\ R_i]^\mathsf{T}$,where ϑ_i is the mean temperature in °C, $p_{\mathrm{PAW},i}$ is the plant-available water in mm, and R_i is the artificial radiation in $\frac{\mathrm{MJ}}{\mathrm{m^2\,d}}$ on day i. The state-space model can then be written as

$$\boldsymbol{x}_{i+1} = \boldsymbol{f}(\boldsymbol{x}_i, \boldsymbol{u}_i), \tag{1}$$

with $\boldsymbol{x}_i$ the state and $\boldsymbol{u}_i$ the input on day i. For a specification of $\boldsymbol{f}$, see (Zhao et al., 2019).

The plant-available water $p_{\mathrm{PAW},i}$ depends on the aridity status of the soil, which directly affects plant growth. For a conversion, the ARID method of Woli et al. (2012) is used, which is based on the FAO Penman-Monteith equations (Allen et al., 1998). The drought is defined as

$$D_i = \begin{cases} 1 - \frac{0.096\ p_{\mathrm{PAW},i}}{ET_{o,i}}, & \text{if } p_{\mathrm{PAW},i} < \frac{ET_{o,i}}{0.096}\ , \\ 0, & \text{otherwise.} \end{cases} \tag{2}$$

If the soil is too dry ($D_i > 0$), the plant suffers from drought stress. The reference crop evapotranspiration $ET_{o,i}$ is given for a uniform grass reference surface. Evapotranspiration means the combination of the evaporation of the soil and the transpiration through the plant itself. It is defined as

$$ET_{o,i} = \frac{0.408\ \delta_i\ R_{n,i} + \gamma\ \frac{900}{\vartheta_i + 273.15}\ \mu_2\ (e_{s,i} - e_{a,i})}{\delta_i + \gamma(1 + 0.34\mu_2)}, \tag{3}$$

where $R_{n,i}$ is the net radiation, γ the psychrometric constant, μ_2 the wind speed, $e_{s,i}$ the saturation vapour pressure, $e_{a,i}$ the actual vapour pressure, δ_i the slope of vapour pressure for each day i. Details can be found in (Allen et al., 1998). The required plant-available water therefore depends on temperature and radiation.

2.2 Dynamic Soil-Moisture Model for Drip Irrigation

The two-dimensional soil-moisture model developed by Romashchenko et al. (2016) describes the movement of water through soil over time given drip irrigation. It can therefore be used to design an irrigation controller and to evaluate the uniformity of the moisture distribution. This section will discuss the mathematical model for the soil and a discrete formulation of the three-dimensional extension of it. Additionally, the phenomenon of evaporation is added. In the following equations, the constant μ is an empirical parameter and therefore has to be found experimentally (Romashchenko et al., 2016). In a simulation study on the impact of μ, the simulations converged and showed stable behavior for $\mu = -0.5$. In future work, further experiments will be performed to refine this value for different soil types. The height of capillary rising h_k, describes the height that water can spontaneously wander upwards through the soil. The maximum molecular moisture capacity of the soil is represented by $W^\star$, and the

complete moisture capacity of the soil is represented by m. These parameters are the boundaries of feasible moisture values and vary with the type of soil used. The moisture W is always contained in the range $W^\star < W < m$. These parameters depend on the type of soil and need to be calibrated experimentally.

The plant-available water of the crop model $p_{\mathrm{PAW},i}$ in $\boldsymbol{u}_i$ can be converted into W with

$$W = \frac{p_{\mathrm{PAW},i}}{d} + W_{\mathrm{wilting}}, \tag{4}$$

where d is the depth of the soil in m and the wilting point is W_{wilting} (Kirkham, 2023).

The model considers pressure differences, the water conductivity of the soil, and external effects such as precipitation or irrigation. The piezometric head

$$U(W) = \mu h_k \left(-\ln \left| \frac{W - W^\star}{m - W^\star} \right| \right)^{\frac{1}{3.5}} + z \tag{5}$$

considers the pressure differences and is expressed in m, where z is the depth. The water conductivity of the soil

$$k(W) = K_\Phi \left(\frac{W - W^\star}{m - W^\star} \right)^{3.5} \tag{6}$$

depends on the moisture level and the type of soil, where K_Φ is the filtration coefficient and assumed to be $0.000075 \frac{\mathrm{m}}{\mathrm{s}}$. Following this definition, its first derivative is defined as

$$k'(W) = 3.5 K_\Phi \left(\frac{1}{m - W^\star} \right)^{3.5} (W - W^\star)^{2.5} \tag{7}$$

leading to a complete description of the model.

Continuous-Time Formulation The change of moisture over time

$$\begin{aligned} \frac{\partial W}{\partial t} = {} & k'(W) \left(\frac{\partial U}{\partial x}\frac{\partial W}{\partial x} + \frac{\partial U}{\partial y}\frac{\partial W}{\partial y} + \frac{\partial U}{\partial z}\frac{\partial W}{\partial z} \right) \\ & + k(W) \left(\frac{\partial^2 U}{\partial x^2} + \frac{\partial^2 U}{\partial y^2} + \frac{\partial^2 U}{\partial z^2} \right) + u_{\mathrm{w}}(x, y, z), \end{aligned} \tag{8}$$

as introduced in (Romashchenko et al., 2016) for two dimensions, incorporates all previously defined functions. The input of the system is given as $u_{\mathrm{w}}(x, y, z)$, and represents the irrigation in this case. While this soil model can be used for simulation purposes, it does not take into account the water loss through evaporation in its original form. Hence, the evaporation is subtracted from the top layer, assuming it follows the definition of (3).

Discretization To allow for a simulation of the model, the equations are discretized, i.e., the soil is split into small volumes, each of them measuring $\Delta x \cdot \Delta y \cdot \Delta z$, and time will be simulated in discrete time steps Δt. The discretized moisture is denoted as W_{ijk} where i, j, and k represents the partition in x, y, and z direction, respectively. The dynamic soil model (8) requires a discrete description of all derivatives included in the model. The first derivatives were discretized using the central difference yielding

$$\frac{\partial U}{\partial x} \approx \frac{U(W_{(i+1)jk}) - U(W_{(i-1)jk})}{2\Delta x}, \tag{9}$$

the first order partial derivative for x of the function $U(W)$. Following this definition, the first-order partial derivative for y and z can be described in the same manner. The first derivative of the moisture W in x-direction, also expressed using the central difference quotient, is

$$\frac{\partial W}{\partial x} \approx \frac{W_{(i+1)jk} - W_{(i-1)jk}}{2\Delta x}, \tag{10}$$

with the first-order discrete derivative for y and z being structured in the exact same way. The second derivatives can be approximated using the second-order difference quotient stated in (Yoshikawa, 2017), resulting in the discrete version of the second derivative of $U(W)$ for x

$$\frac{\partial^2 U}{\partial x^2} \approx \frac{U(W_{(i+1)jk}) - 2U(W_{ijk}) + U(W_{(i-1)jk})}{(\Delta x)^2} \tag{11}$$

depending on the current value and the values of the spatial predecessor and successor. The definitions for y- and z-direction follow the same form.

3. HIERARCHICAL SET-POINT IRRIGATION CONTROL

This section introduces the two-level hierarchical control method for irrigation. At the higher level of the hierarchy, set-points for an underlying PID controller are determined by solving an offline open-loop OCP that finds the optimal plant-available water for each day to maximize crop growth and minimize cost. This is described in Section 3.1. The lower-level online control is based on a PID controller that tracks these set-points. The design of the PID controller is presented in Section 3.2.

3.1 Optimal Control for Vertical Farming

The set-point optimization is based on a cost function

$$J(\boldsymbol{U}, \boldsymbol{x}_0) = \sum_{i=0}^{N-1} l(\boldsymbol{u}_i) - V(\boldsymbol{x}_N) \tag{12}$$

that is defined over a given growth period of N days. With $\boldsymbol{U} = \left[\boldsymbol{u}_0^\mathsf{T}, \boldsymbol{u}_1^\mathsf{T}, ..., \boldsymbol{u}_{N-1}^\mathsf{T}\right]^\mathsf{T}$, the input sequence is denoted. The stage cost $l(\boldsymbol{u}_i)$ represents the energy cost used for the growing process and is given as $l(\boldsymbol{u}_i) = \boldsymbol{u}_i^\mathsf{T} \boldsymbol{R} \boldsymbol{u}_i + \boldsymbol{r}^\mathsf{T} \boldsymbol{u}_i$, where $\boldsymbol{R}$ and $\boldsymbol{r}$ are weights. The terminal cost $V(\boldsymbol{x}_N)$ gives the yield at harvest on day N. The price evolves linearly, leading to a linear cost term, i.e., $V(\boldsymbol{x}_N) = \boldsymbol{q}^\mathsf{T} \boldsymbol{x}_N$, with the weight $\boldsymbol{q}$. The cost function (12) represents the negative economic yield. Thus, the terminal cost is used with a negative sign. Temperature, plant-available water, and radiation can be controlled in a VF, but their values are bounded. Therefore, constraints $\boldsymbol{u}_i \in \mathcal{U}$ are added to the OCP. These considerations yield the OCP

$$\begin{aligned} \boldsymbol{U}^* = {} & \arg\min_{\boldsymbol{U}} J(\boldsymbol{U}, \boldsymbol{x}_0) && && \text{(13a)} \\ \text{s.t. } & \boldsymbol{x}_{i+1} = \boldsymbol{f}(\boldsymbol{x}_i, \boldsymbol{u}_i) && \forall i \in [0, N-1] && \text{(13b)} \\ & \boldsymbol{u}_i \in \mathcal{U} && \forall i \in [0, N-1] && \text{(13c)} \\ & \tau_N > \tau_{\mathrm{mature}} && && \text{(13d)} \\ & \boldsymbol{x}_0 = \boldsymbol{x}_{\mathrm{init}}, && && \text{(13e)} \end{aligned}$$

where $\boldsymbol{U}^*$ is the sequence of optimal inputs. The states on day $i = 0$ are given as initial states $\boldsymbol{x}_{\mathrm{init}}$. The system model

$\boldsymbol{f}$ refers to (1). Maturity of the crop is ensured through $\tau_N > \tau_{\text{mature}}$, where τ_{mature} is a parameter depending on the chosen crop. OCP (13) can be solved using standard nonlinear optimization solvers.

3.2 PID Controller Design

The PID controller for moisture control is designed in z-direction only. Moisture is measured in the layer z_{root} below the irrigation points, and an individual PID controller is used for each irrigation point. A number of independent controllers and irrigation points are used to achieve a uniform moisture distribution in the defined soil volume.

Linearization of the Soil Model in z-Direction The PID controller uses the measurement of the moisture value at the depth of the roots z_{root} under the irrigation point as feedback information. The influences of changes in the x and y direction are neglected, which simplifies (8) to

$$\frac{\partial W}{\partial t} = k'(W)\frac{\partial U}{\partial z}\frac{\partial W}{\partial z} + k(W)\frac{\partial^2 U}{\partial z^2} + u_{\text{w}}(z), \tag{14}$$

where the input of the irrigation $u_{\text{w}}(z)$ is zero for all $z \neq 1$, meaning only the top layer $z = 1$ is irrigated. A spatial discretization in z-direction results in a z_{root} dimensional state space with the state vector $\mathbf{W} = [W_1\ W_2\ \dots\ W_{z_{\text{root}}}]^\top$. The linearization of (14) around the desired moisture results in a linear system for the moisture values, i.e.,

$$\frac{d\mathbf{W}}{dt} = A\mathbf{W} + Bu\,, \tag{15a}$$

$$W_{z_{\text{root}}} = C\mathbf{W}\,, \tag{15b}$$

where $B = [1\ 0\ 0...]^\top$ and $C = [0\ ..\ 0\ 1]$. The input in (14) is only applied on the top layer as the change of the relative moisture in that point, resulting in a one-dimensional input u for each irrigation point.

State Space System for PID Tuning In this study, moisture is measured in the 5-th layer of the discretization, yielding the system matrix

$$A = \begin{bmatrix} -0.18 & 0.18 & 0. & 0. & 0. \\ 0.21 & -0.4 & 0.18 & 0. & 0. \\ 0. & 0.21 & -0.4 & 0.18 & 0. \\ 0. & 0. & 0.21 & -0.4 & 0.18 \\ 0. & 0. & 0. & 0.21 & -0.21 \end{bmatrix}. \tag{16}$$

From the state space model, a transfer function is determined that can then be used to tune the PID controller using an arbitrary PID tuning technique. Here, the MATLAB toolbox (Wang, 2020) is used to tune the controller to a crossover frequency of $\frac{1}{10\text{min}}$ resulting in the PID gains

$$K_p = 0.00617, \tag{17a}$$

$$K_i = 1.72 \cdot 10^{-6},\ \text{and} \tag{17b}$$

$$K_d = 0.302. \tag{17c}$$

The PID controller uses the reference value $W_{z_{\text{root,des}}}$, which is derived from the result of (13) for the plant-available water $p_{\text{PAW},i}$ and is transformed with (4). To achieve these reference values at the measuring points, it determines the suitable values for u.

4. RESULTS

4.1 Results for Set-Point Trajectory

The results for the set-point optimization conducted with CasADi (Andersson et al., 2019) are presented for a wheat crop grown over 130 days, considering the cost

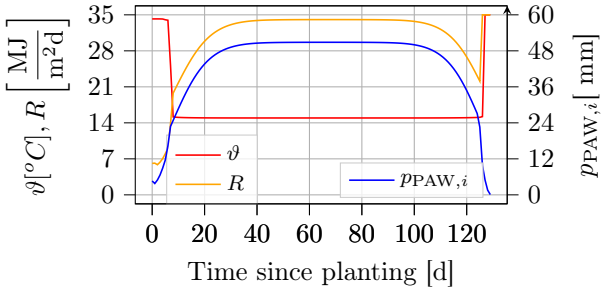

Fig. 1. Optimal inputs trajectory that can be used as daily set-points.

parameters of $\mathbf{R} = \begin{bmatrix} 1.86{\cdot}10^{-6} & 0 & 0 \\ 0 & 0.2 & 0 \\ 0 & 0 & 0 \end{bmatrix}$, $\mathbf{q} = \begin{bmatrix} 3600 \\ 0 \\ 0 \end{bmatrix}$, and $\mathbf{r} = \begin{bmatrix} -3.73{\cdot}10^{-5} \\ 0.04 \\ 0.04 \end{bmatrix}$. The following assumptions about the environment are made to limit the complexity of the optimal control approach discussed in Section 3.1. As the CO_2 concentration in the atmosphere has no direct influence on the irrigation set-points, given this model, it is set to a constant value of $C_{\text{CO}_2,i} = 350$ ppm. A reasonably good temperature control is assumed such that there are no temperature peaks during the day, i.e., the mean and maximum temperatures are the same. Furthermore, a constant humidity of 60% as well as a small wind speed of $\mu_2 = 0.2\,\frac{\text{m}}{\text{s}}$ are assumed. The outside temperature is set to a constant value of 10 °C, making active cooling in the VF unnecessary. The common assumption of soil heat flux density being negligible is adopted here. These variables can easily be added to the optimization if needed.

One can observe the interdependence of the inputs in Fig. 1, which influence the corresponding states shown in Fig. 2. Initially, it is most cost-effective to start with a low moisture level, indicating minimal plant-available water ($p_{\text{PAW},i}$). This is due to the low evapotranspiration given the low radiation levels. The optimization strategy avoids scenarios where high radiation and temperature produce exceptionally high evapotranspiration. Only when the temperature decreases, and the radiation increases, does the plant require more water, which corresponds to a significant increase in transpiration. The required plant-available water stabilizes at nearly 50 mm per day, implying that plant and soil evaporation collectively amount to approximately $0.096 \cdot 50$ mm $= 4.8$ mm per day. Towards the end, as wheat matures and dries, both temperature and radiation increase, eliminating the need for further irrigation. Ultimately, a biomass of 4.13 $\frac{\text{kg}}{\text{m}^2}$ can be achieved, with the potential for significant improvement with a higher $C_{\text{CO}_2,i}$.

4.2 Soil Dynamics Simulation

The soil is simulated with 1500 spatially discretized elements ($n_x = n_y = 10$, n_z=15), where the discretization step is uniform, $\Delta x = \Delta y = \Delta z = 0.02$ m. The moisture is limited by $W^\star = 0.15$ and $m = 0.35$. The height of the capillary rise is $h_k = 1.25$ m, representing sandy soil. The parameters were adopted from the calibrated soil conditions from Zhao et al. (2019) and Romashchenko et al. (2016).

4.3 Results for PID Control

As an example, the moisture dynamics are shown for day 8 of the optimized trajectory, where $p_{\text{PAW},i} = 24$ mm

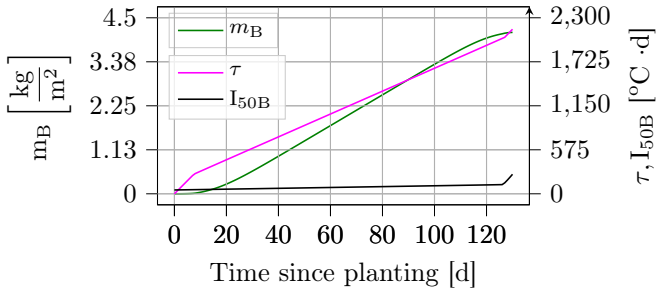

Fig. 2. Optimal states corresponding to the optimal inputs for every day.

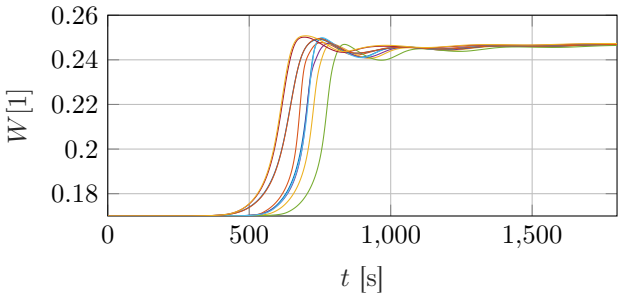

Fig. 3. Moisture trajectory for each measurement point, in the z_{root}-th layer below the irrigation points. Each measurement point (out of 10 measurement points) is denoted with a different color.

is needed for optimal growth. With the wilting point of $W_{\text{wilting}} = 0.17$, this results in the desired moisture of $W_{z_{\text{root,des}}} = 0.25$ for each of the 10 irrigation points. For the distribution of the ten irrigation points, the Centroidal Voronoi Tessellation algorithm (Du et al., 1999) is chosen for its superior performance compared to a regular grid distribution. The distribution of the irrigation points can be seen in Fig. 5 after 60 s, where the irrigation points are the only points with $W > 0.2$. The initial state of the soil moisture is set to 0.17 representing almost dry soil and serving as a somewhat worst-case scenario. The moisture sensors are assumed to be placed at $z_{\text{root}} = 0.1$ m.

Fig. 3 illustrates that it takes more than 450 s for the added moisture to reach the sensors in the z_{root}-th layer, even after the irrigation has started. The desired moisture $W_{z_{\text{root,des}}}$ is reached for all measuring points after approximately 800 s (13 min), which corresponds to the PID design. In Fig. 4, the inputs u for the irrigation points are shown in $\frac{\text{l}}{\text{h}}$. After reaching the desired moisture $W_{z_{\text{root,des}}}$, the inputs remain at small values. The reason for this is illustrated in Fig. 5, which shows the moisture content of a soil block in different time steps. After 1200 seconds, the soil in some parts has reached the desired moisture level, but the lower part of the soil block remains dry. As a result, additional water is required until the entire block, up to the root depth z_{root}, is uniformly moist. This is accomplished after one hour. After that, the controller will only replace the water lost through evapotranspiration and drainage to deeper layers.

5. DISCUSSION

In this paper, our focus has been on integrating an irrigation control scheme into the overall optimal control framework for a VF. The optimal trajectory is computed offline, and subsequently, a PID controller is employed to track this trajectory. The performance of this hierarchical approach has demonstrated remarkable results in simulation. While this hierarchical structure already shows very promising results, it could be extended to a closed-loop approach in higher levels of plant dynamics control. This ensures good performance also if the lower-level PID controller struggles to achieve perfect trajectory tracking, resulting in suboptimal overall trajectories. Moreover, the growing time for the wheat crop in this study has been set to 130 days. The entire approach can be embedded into an OCP with free final time, as demonstrated in previous work (Daniels et al., 2023). Additionally, it was observed that a high number of irrigation points in a small area can achieve a uniform moisture distribution in a short time. While advantageous for uniform crop growth, the high number of irrigation points may incur high costs and maintenance efforts. Therefore, it would be beneficial to investigate the optimal number and distribution of irrigation points when precise settings and costs are known. An alternative approach to many sensors could be the use of virtual sensors with more accurate evapotranspiration models, as demonstrated by Sánchez et al. (2012), providing a potentially simpler measurement system and a better estimate of the actual evapotranspiration ET depending on the type of crop and its growth.

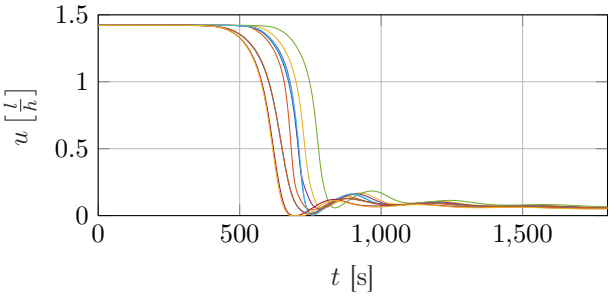

Fig. 4. Input trajectory for each irrigation point, given in liters per hour. The input trajectories (for the 10 irrigation points) have the corresponding colors to the measurement points in Fig. 3.

6. CONCLUSION

A hierarchical approach for irrigation in a vertical farm has been presented. An OCP is first solved offline to obtain a trajectory for the optimal amount of water in soil for each day, considering plant growth and energy consumption. A subordinate control loop, which consists of several PID controllers, adjusts the water supply to stabilize the given trajectory given a dynamic soil model for drip irrigation. Our results provide a successful proof of concept through a comprehensive simulation study. These results not only confirm the feasibility of our approach, but also demonstrate its potential for practical application in vertical farming. Future work will include an experimental validation of our findings and the extension to a closed-loop crop control system for all inputs.

REFERENCES

Abioye, E.A., Abidin, M.S.Z., Mahmud, M.S.A., Buyamin, S., Ijike, O.D., Otuoze, A.O., Afis, A.A., and Olajide,

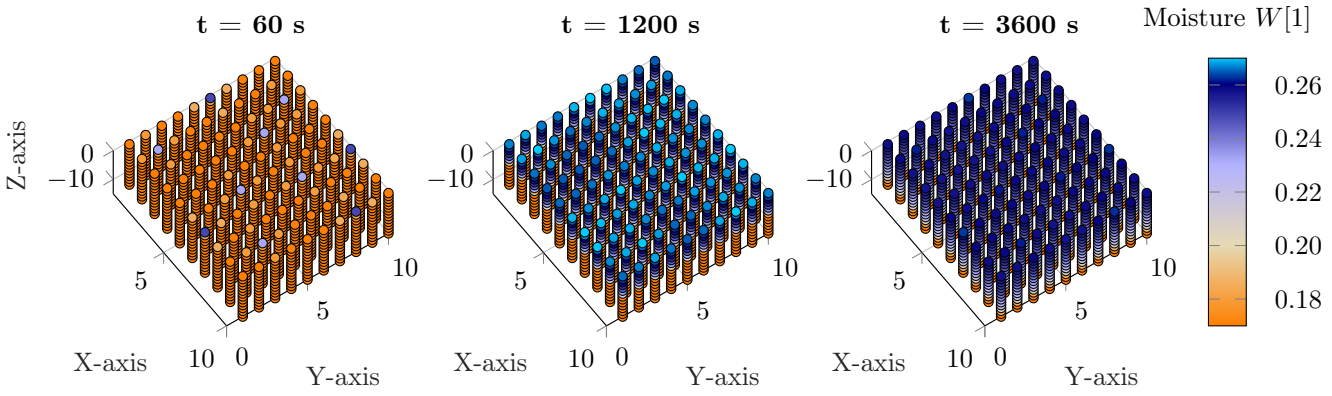

Fig. 5. Moisture W in a block of soil at different time steps: 60 s (1 min), 1200 s (20 min) and 3600 s (1 h). The desired moisture is $W_{z_{\text{root,des}}} = 0.25$.

O.M. (2023). A data-driven Kalman filter-PID controller for fibrous capillary irrigation. *Smart Agric. Technol.*, 3, 100085.

Allen, R.G., Pereira, L.S., Raes, D., Smith, M., et al. (1998). Crop evapotranspiration-guidelines for computing crop water requirements-FAO irrigation and drainage paper 56. *Fao, Rome*, 300(9), D05109.

Andersson, J., Gillis, J., Horn, G., Rawlings, J., and Diehl, M. (2019). CasADi – A software framework for nonlinear optimization and optimal control. *Math. Program. Comput.*, 11(1), 1–36.

Bender, S.F., Wagg, C., and van der Heijden, M.G. (2016). An underground revolution: biodiversity and soil ecological engineering for agricultural sustainability. *Trends Ecol. Evol.*, 31(6), 440–452.

Cáceres, G., Millán, P., Pereira, M., and Lozano, D. (2021). Smart farm irrigation: Model predictive control for economic optimal irrigation in agriculture. *Agron. J.*, 11(9), 1810.

Cáceres, R., Casadesús, J., and Marfà, O. (2007). Adaptation of an automatic irrigation-control tray system for outdoor nurseries. *Biosyst. Eng.*, 96(3), 419–425.

Daniels, A., Fink, M., Leibold, M., Wollherr, D., and Asseng, S. (2023). Optimal control for indoor vertical farms based on crop growth. *IFAC-PapersOnLine*, 56(2), 9887–9893.

Du, Q., Faber, V., and Gunzburger, M. (1999). Centroidal voronoi tessellations: Applications and algorithms. *SIAM review*, 41(4), 637–676.

Fink, M., Daniels, A., Qian, C., Velásquez, V.M., Salotra, S., and Wollherr, D. (2023). Comparison of dynamic tomato growth models for optimal control in greenhouses. In *IEEE AGRETA*, 28–33.

Graamans, L., Baeza, E., Van Den Dobbelsteen, A., Tsafaras, I., and Stanghellini, C. (2018). Plant factories versus greenhouses: Comparison of resource use efficiency. *Agric. Syst.*, 160, 31–43.

Hassan, S.I., Alam, M.M., Illahi, U., Al Ghamdi, M.A., Almotiri, S.H., and Su'ud, M.M. (2021). A systematic review on monitoring and advanced control strategies in smart agriculture. *IEEE Access*, 9, 32517–32548.

Kirkham, M.B. (2023). *Principles of soil and plant water relations*. Elsevier.

Muñoz-Carpena, R. and Dukes, M.D. (2005). Automatic irrigation based on soil moisture for vegetable crops: Abe356/ae354, 6/2005. *EDIS*, 2005(8).

Ortega Álvarez, J.F., de Juan Valero, J.A., Tarjuelo Martín-Benito, J.M., and López Mata, E. (2004). Mopeco: an economic optimization model for irrigation water management. *Irrig. Sci.*, 23, 61–75.

Puig, F., Rodríguez Díaz, J.A., and Soriano, M.A. (2022). Development of a low-cost open-source platform for smart irrigation systems. *Agron. J.*, 12(12), 2909.

Rodríguez, F., Berenguel, M., Guzmán, J.L., and Ramírez-Arias, A. (2015). Crop growth control. In *Modeling and Control of Greenhouse Crop Growth*, 197–214. Springer.

Romashchenko, M., Shatkovsky, A., and Onotsky, V. (2016). Mathematical model of flat-vertical profile moisture transfer under trickle irrigation in conditions of incomplete saturation. *Agric. sci. pract.*, 3(3), 35–40.

Romero, R., Muriel, J., García, I., and de la Peña, D.M. (2012). Research on automatic irrigation control: State of the art and recent results. *Agric. Water Manage.*, 114, 59–66.

Romero, R. (2011). Hydraulic modelling and control of the soil-plant-atmosphere continuum in woody crops. *PhD Thesis*.

Sánchez, J.A., Rodríguez, F., Guzmán, J.L., and Arahal, M.R. (2012). Virtual sensors for designing irrigation controllers in greenhouses. *Sensors*, 12(11), 15244–15266.

Sheikh, S.S., Javed, A., Anas, M., and Ahmed, F. (2018). Solar based smart irrigation system using PID controller. In *IOP Conf. Ser.: Mater. Sci. Eng.*, volume 414, 012040. IOP Publishing.

Trivedi, P., Leach, J.E., Tringe, S.G., Sa, T., and Singh, B.K. (2020). Plant–microbiome interactions: from community assembly to plant health. *Nat. Rev. Microbiol*, 18(11), 607–621.

Wang, L. (2020). *PID control system design and automatic tuning using MATLAB/Simulink*. John Wiley & Sons.

Woli, P., Jones, J.W., Ingram, K.T., and Fraisse, C.W. (2012). Agricultural reference index for drought (ARID). *J. Agron.*, 104(2), 287–300.

Yoshikawa, S. (2017). Energy method for structure-preserving finite difference schemes and some properties of difference quotient. *J. Comput. a. Appl. Math.*, 311, 394–413.

Zhao, C., Liu, B., Xiao, L., Hoogenboom, G., Boote, K.J., Kassie, B.T., Pavan, W., Shelia, V., Kim, K.S., Hernandez-Ochoa, I.M., et al. (2019). A SIMPLE crop model. *Eur. J. Agron.*, 104, 97–106.